Quaternary Science Reviews 254 (2021) 106799

Contents lists available at ScienceDirect

Quaternary Science Reviews

journal homepage: www.elsevier.com/locate/quascirev

Assessing proxy system models of cave dripwater $\delta^{18}O$ variability

Jun Hu [a, *], Sylvia G. Dee [a], Corinne I. Wong [b], Ciaran J. Harman [c, d], Jay L. Banner [b], Kendra E. Bunnell [b]

[a] Department of Earth, Environmental, and Planetary Sciences, Rice University, Houston, TX, 77098, USA
[b] Department of Geological Sciences, The University of Texas at Austin, Austin, TX, 78712, USA
[c] Department of Environmental Health and Engineering, Johns Hopkins University, Baltimore, MD, 21218, USA
[d] Department of Earth and Planetary Science, Johns Hopkins University, Baltimore, MD, 21218, USA

ARTICLE INFO

Article history:
Received 15 May 2020
Received in revised form
23 November 2020
Accepted 10 January 2021
Available online 1 February 2021

Handling Editor: Mira Matthews

Keywords:
Speleothems
Paleoclimatology
Proxy system models
Stable isotopes
Quaternary
North America
Global

ABSTRACT

Large uncertainties in future climate change necessitate understanding of decadal-centennial variability in past climate. Speleothems, which capture changes in the stable isotope composition (i.e., $\delta^{18}O$ values) of rainfall, have been widely employed to constrain hydroclimate variability in the past due to their continuous growth and potential for high temporal resolution. However, the interpretation of speleothem proxies (i.e., geochemical and growth rate records) is still imperfectly constrained. One challenge involves understanding the transformation from rainfall $\delta^{18}O$ to calcite $\delta^{18}O$. A recent advance to address this challenge is the development of proxy system models (PSMs), which translate climate variables to speleothem calcite $\delta^{18}O$ values. However, the complexity and applicability of each model varies. In order to assess which speleothem PSMs are most suitable for simulating speleothem records, we evaluate four commonly applied PSMs, which span a range of complexity (one simple, two intermediate-complexity, and one complex model). The evaluation is based on a given model's ability to simulate observed drip $\delta^{18}O$ time series using multi-year long cave dripwater and rainfall data sets from semi-arid central Texas and tropical Borneo. The models are based on the running mean of rainfall $\delta^{18}O$ (RM model), dripwater transit time (PRYSM model), StorAge Selection (SAS model), and combination of flow paths in karst systems (Karstolution model). We explore the parameter settings of these models and evaluate them employing the Root Mean Square Errors (RMSEs) metric. We find that for drip sites in semi-arid climates with long residence times, model complexity of at least intermediate levels is required to simulate cave dripwater $\delta^{18}O$ variability. The RMSEs of intermediate-complexity PSMs (PRYSM, SAS, and Karstolution) are close to the range of analytical errors, while the RMSE of the simple RM model is far larger. For drip sites in wet climates with short residence times, all four models, including the RM model, are capable of simulating cave dripwater $\delta^{18}O$ well. In practice, we assert that the use of models of intermediate complexity such as PRYSM may be required when detailed knowledge of variables such as groundwater residence time for a given cave setting is unknown. Such PSMs are useful for global-scale studies due to their broad applicability and simplicity. We also illustrate the use of comprehensive physical models, such as Karstolution, for understanding cave processes like fractionation due to epikarst evaporation. The poorer performance of the PSMs in semi-arid environments than their performance in humid environments suggests that additional in-situ process studies are needed to improve simulations of relatively dry cave systems and provide enhanced interpretations of speleothem reconstructions from these environments.

1. Introduction

The future response of the hydrologic cycle to climate change has critical implications for society, including food security, energy production, and human health. Forecasting future hydroclimate necessitates a comprehensive understanding of the links between climate and the hydrologic cycle, which can be illuminated through the study of past climate. Our understanding of past climate variability will be advanced by integrating paleoclimate data and

* Corresponding author.
E-mail address: jun.hu@rice.edu (J. Hu).

https://doi.org/10.1016/j.quascirev.2021.106799
0277-3791/

paleoclimate modeling approaches. This requires the interpretation of past climate from a climate archive (e.g., ice cores, sedimentary rocks, tree rings, speleothems) (Evans et al., 2013; Dee et al., 2015a). The accurate interpretation often necessitates nuanced knowledge of the links between climate and proxy variability as well as the processes affecting the preservation of proxy in each archive, and potentially, at each site. Studies that draw on proxies from multiple archives, therefore, need to tap an increasingly broad range of expertise and may ultimately result in overgeneralized interpretations. In contrast, Proxy System Models (PSMs) facilitate the translation of climate data into proxy data, allowing a piecewise evaluation of climate signal transfers. PSMs will ideally make proxy data more useable to the broader scientific community and generate greater consistency in data-model comparison methods across studies, including those that integrate global data sets (e.g., Baker et al., 2019; James et al., 2015). To this end, this study focuses on PSMs for cave dripwater $\delta^{18}O$, which determines speleothem calcite $\delta^{18}O$ values.

Speleothems are mineral deposits (principally calcite) formed in caves and have been widely used to investigate past hydroclimate variability, such as monsoon variability and glacial terminations over orbital to interannual timescales (Bar-Matthews et al., 1999; McDermott, 2004; Wang et al., 2001, 2008; Cheng et al., 2009, 2012, 2016; Carolin et al., 2013, 2016). Speleothems afford high dating precision (approaching ±0.1% of estimated ages) (Cheng et al., 2013) and high temporal resolution. Thus, speleothems offer data-rich archives for constraining hydroclimate variability in the past.

The translation of rainfall $\delta^{18}O$ into speleothem calcite $\delta^{18}O$ values can be compartmentalized into two steps: (1) transformation of rainfall to cave dripwater $\delta^{18}O$ values, and (2) preservation of cave dripwater $\delta^{18}O$ values in speleothem calcite (Baker et al., 2013; Wong and Breecker, 2015). In this study, we focus on the former since we have multi-year long cave dripwater data but without concurrent speleothem calcite data for all study regions. (Indeed, we acknowledge that the second step is important and cannot be neglected when interpreting speleothem $\delta^{18}O$.) Cave dripwater $\delta^{18}O$ variability is dampened relative to that of local precipitation due to attenuation of high precipitation events and mixing of relatively young and old water in the vadose zone above the cave. Further, cave dripwater $\delta^{18}O$ values may be biased toward a season of preferential recharge or preferential speleothem growth (James et al., 2015) or get elevated following evaporation during infiltration. There have been extensive efforts to understand the impact of karst processes on speleothem records by both cave monitoring and modeling. Monitoring is widely used to estimate drip types, residence time of dripwater, growth rate of speleothem, and other key parameters for one cave or global caves (Moerman et al., 2014; James et al., 2015; Duan et al., 2016; Baker et al., 2019). On the other hand, spatial and temporal variability in cave dripwater $\delta^{18}O$ values are modeled using both empirical and conceptual approaches. There are various iterations of a conceptual, lumped parameter hydrologic model based on single and multiple, interconnected linear reservoirs (Gelhar and Wilson, 1974; Wackerbarth et al., 2010; Kirchner et al., 2001; Partin et al., 2013; Baker et al., 2013; Dee et al., 2015a; Hartmann et al., 2014; Treble et al., 2019). These models represent hydrological processes that offer explanatory insight but often require extensive parameterization. Empirical methods typically involve the convolution of precipitation $\delta^{18}O$ time series, require less extensive parameterization, and have high predictive power when trained with sufficient data. However, the explanatory depth of empirical methods is limited because model constraints are weakly related to the characteristics and processes of the system. For example, the transit time of dripwater is related to the usually unknown flow paths within a cave. This study focuses primarily on empirical approaches, which are categorized as PSMs of intermediate complexity (IC). Such IC models strike a balance between accessibility and providing a representation of reality.

Here, we test the performance of several of these approaches using two decade-long cave dripwater data sets from semi-arid central Texas, USA (Pape et al., 2010; Feng et al., 2014; Hulewicz, 2015; Bunnell, 2019) and Borneo, Malaysia (Moerman et al., 2014; Ellis et al., 2020) that span multiple cycles of wet and dry conditions. Although previous work has developed approaches for modeling the temporal variability of cave dripwater $\delta^{18}O$ values, the performance of these methods has yet to be assessed in contrasting environmental settings.

Precipitation-amount-weighted averaging of the precipitation $\delta^{18}O$ time series was successfully used to characterize seven years of cave dripwater $\delta^{18}O$ in tropical Borneo (Moerman et al., 2014). Meanwhile, Dee et al. (2015a) proposed a simple convolution of the precipitation $\delta^{18}O$ time series with dripwater transit time distributions (i.e., the probability density function of the age of a population of water parcels exiting a system) in their PRoxY System Model (PRYSM) open-source framework. An additional approach, StorAge Selection (SAS) (Harman, 2015), quantifies transit time distributions using functions that represent the way storage (ranked by age) is selected and released to discharge. SAS accounts for the effect of antecedent moisture conditions on shifts in flow pathways and connectivity that determine the age distribution of water exiting a system. Finally, we evaluate a high-complexity, physics-based speleothem model, Karstolution (Treble et al., 2019), which is a multiple-component model employing several flow pathways amongst water stores in karst systems. Our objectives are to i) evaluate the added benefit of increased complexity in each setting, and ii) provide an overview of the strengths and weaknesses of each model, and thus guidelines for selecting an appropriate PSM in paleoclimate studies.

2. Methods

2.1. Data

We expand cave dripwater $\delta^{18}O$ datasets at two central Texas caves, Inner Space Cavern (IS) and Natural Bridge Caverns (NB) (Pape et al., 2010; Feng et al., 2014; Hulewicz, 2015; Bunnell, 2019), and a precipitation $\delta^{18}O$ dataset following the methods of Pape et al. (2010). The integrated dataset is shown in Table S1 (note the new data in this study spans the period 2007 to 2014; the "Source" column of Table S1 gives references for the source of each data point). Dripwater was collected every 4–6 weeks from 1999 through 2018 at multiple drip sites in IS and from 1999 to 2014 in NB, and bulk precipitation was collected approximately monthly. Water was collected in glass vials without headspace. Rainwater samples were collected employing a layer of mineral oil to limit evaporation and were filtered before analysis. At the time of collection, plastic (HDPE) vials were also filled for other analyses. Plastic vials contained variable amounts of headspace depending on volume limitations. All vials were sealed with Parafilm and archived in refrigerated conditions.

The two Texas caves are located in areas where the climate transitions from sub-humid to semi-arid. Summers are hot and winters are mild. The annual average rainfall is 789 mm and 915 mm at NB and IS, respectively, but can vary significantly from year to year (200–1500 mm) as the region frequently cycles through extreme wet and dry periods. The caves developed in the Edwards Plateau, which is a regionally extensive karstified Cretaceous carbonate platform. Drip sites are overlain by 40–60 m of bedrock at NB and 20 m of bedrock at IS. Vegetation consists of savanna with interspersed woodland patches, and soils are thin,

averaging 20 cm.

We focus on two sites in each cave that represent dominantly diffuse vs. conduit supplied drips based on drip rate variability, where diffuse (conduit) sites are characterized by a low (high) maximum drip rate and low (high) coefficient of variation. The drip rates of sites NBSB and ISSR3 have coefficients of variation >50% and are thus categorized as conduit-type sites (or seasonal drip sites) (Smart and Friederich, 1986; Partin et al., 2012). Sites NBBC and ISLM are categorized as diffuse-type sites (or seepage flow sites). Measurements of cave dripwater $\delta^{18}O$ values were conducted using a Gas Bench Inlet interface to a MAT 253 Gas Isotope Ratio Mass Spectrometer in the Stable Isotope and Paleoclimate Analysis (SPA) Lab at Skidmore College (Table S1). The precision of the internal water standard analyzed at the SPA Lab was better than 0.14‰ for $\delta^{18}O$ (n = 11), based on twice the standard error. The average offset between replicate analyses of sample duplicates in the SPA Lab was 0.2‰ based on the measurement of 32 paired analyses of $\delta^{18}O$. Water collected in HDPE vials was analyzed in cases where glass vials broke due to freezing during shipment to the SPA lab. Comparisons (n = 4) of water sampled in glass and HDPE at the same site and time documented offsets between water collected and stored in glass and HDPE vials to be between 0.1 and 0.2‰ for $\delta^{18}O$. In this manuscript, the precision of the dataset is conservatively estimated to be ±0.3‰ for $\delta^{18}O$, based on half the 95th percentile of replicate offset values. Finally, the offsets of $\delta^{18}O$ between the previously measured and re-analyzed samples at the SPA laboratory mostly (10 of 11 samples) fall into this uncertainty range for $\delta^{18}O$.

Precipitation data were collected every 4–6 weeks over the same time interval from the rooftop of the Jackson Geology Building at the University of Texas at Austin (UT), which is located between the cave sites. The average annual rainfall in the region over the time period 1999–2018 is approximately 884 mm. Measurements of precipitation $\delta^{18}O$ values (n = 10) were conducted to infill the existing precipitation stable isotope data set using a Gas Bench Inlet interface to a MAT 253 Gas Isotope Ratio Mass Spectrometer in the Stable Isotope Lab for Critical Zone Gases at The University of Texas, Austin. The $\delta^{18}O$ values of water standards in this laboratory were reproducible within ±0.1‰ (1σ). Rainfall amount data at UT (daily) is represented by the Camp Mabry station rainfall data from the Global Historical Climatology Network (GHCN) dataset (Menne et al., 2012). Although we do not have monitoring of rainfall $\delta^{18}O$ of Texas caves, we use rainfall data at UT to represent their rainfall data since they are relatively close to the UT campus (IS is 30 km from UT, and NB is 80 km from UT). Correlations between monthly rainfall amounts at UT, IS, and NB are high (0.79–0.81, significant at the 95% level). As there are limited continuous evapotranspiration data sets from 1999 to 2018, we extract daily evaporation data at UT from the reanalysis dataset The Modern-Era Retrospective analysis for Research and Applications, Version 2 (MERRA-2) (Gelaro et al., 2017). Evaporation in the dataset is mostly soil and canopy evaporation derived from the land surface model – specifically, the Catchment model (Koster et al., 2000) in the MERRA-2 system (Reichle et al., 2017). To investigate how cave dripwater $\delta^{18}O$ imprints hydroclimate variability, we calculated the monthly rainfall anomalies (monthly values minus climatological mean) at the Camp Mabry station.

The third data set, representing a tropical climate, was retrieved from the published cave dripwater and precipitation dataset from northwest Borneo presented in Moerman et al. (2014) and Ellis et al. (2020), which spans the period 2006 to 2018. Dripwater was collected every two weeks from three sites, Wind Fast (WF), Wind Slow (WS), and Lang Second (L2), and precipitation was collected daily. All three drip sites are categorized as diffuse-type based on their low drip rates and variability. The sites are located in a tropical climate with little seasonality in temperature and precipitation, and an annual average precipitation of 5000 mm. The caves developed in a late Eocene to early Miocene shallow marine carbonate platform (Melinau Limestone Formation), and drip sites are overlain by 100 m of bedrock.

2.2. Models

Dripwater $\delta^{18}O$ variability at Texas and Borneo drip sites was forward-modeled using four approaches, which increase from lowest-complexity to highest-complexity. Brief descriptions of the following models are introduced in Table 1 and Figure S1. Models are partitioned into the environment (i.e., climate inputs) and sensor models (i.e., model approaches, which describe proxy's responses to climate forcing) according to Evans et al. (2013). Here, we focus on dripwater $\delta^{18}O$ instead of calcite $\delta^{18}O$; thus, we do not discuss carbonate fractionation, speleothem growth rate, and age uncertainties. We choose the following models because they are widely used in the speleothem community and represent a hierarchy of model complexity/types: a simple weighted-average algorithm, a simple physical model, a travel time distribution model, and a comprehensive physical model.

1. **RM.** The first approach simulates cave dripwater $\delta^{18}O$ by averaging monthly precipitation $\delta^{18}O$ values over the previous n months weighted by monthly rainfall amount (i.e., backward running mean (RM)):

$$\delta^{18}O_{RMi} = \frac{\sum_{m=i}^{i-n+1} \delta^{18}O_m \cdot P_m}{\sum_{m=i}^{i-n+1} P_m} \quad (1)$$

where $\delta^{18}O_{RMi}$ is the simulated $\delta^{18}O$ value of month i, $\delta^{18}O_m$ is monthly precipitation $\delta^{18}O$, P_m is monthly rainfall amount, and n is the number of months for averaging – the only free parameter in the RM model. The monthly precipitation $\delta^{18}O$ is the average of daily rainfall amount-weighted precipitation $\delta^{18}O$. This method is the same as the autogenic model used in Moerman et al. (2014) for simulating dripwater $\delta^{18}O$ in Borneo caves. The number of n months is taken as the residence time of the cave dripwater.

2. **PRYSM** (Dee et al., 2015a). The second approach applies a convolution to the monthly amount-weighted precipitation $\delta^{18}O$ time series with a response function (i.e., a reaction of a system in response to an external change) characterized by the mean transit time of dripwater (Fig. S1) from the surface to the cave, following the approach of Gelhar and Wilson (1974). Conceptually, this approach simulates cave dripwater $\delta^{18}O$ values as a mixture of recharging precipitation $\delta^{18}O$ values, assuming a uniform distribution of water transit time. This approach underlies the speleothem PSM in the open-source framework for PRoxY System Modeling (PRYSM) described in Dee et al. (2015a). PRYSM includes two model options: the well-mixed model (Partin et al., 2013) and advection-dispersion model (Kirchner et al., 2001; Wackerbarth et al., 2010). Both model options assume that precipitation filters into a water store; the subsequent outflow of this water store is cave dripwater (Dee et al., 2015a, 2017). The well-mixed model is mainly dependent on the residence time (τ) of water in that store. In

Table 1
Model descriptions, data inputs and parameters.

Models	Data input	Parameters	How it works
RM	Precipitation $\delta^{18}O$ Precipitation amount	Months to average over	Averaging precipitation $\delta^{18}O$ of neighboring months, weighted by rainfall amount
PRYSM	Precipitation $\delta^{18}O$ Precipitation amount	Average transit time Peclet number (advection-dispersion model)	Convoluting precipitation $\delta^{18}O$ with a response function (depending on the transit time)
SAS	Precipitation $\delta^{18}O$ Precipitation amount Evapotranspiration Drip rate	Shape parameter α Scale parameter λ Mean reservoir storage S_o Initial evapotranspiration storage E_0	Calculating dripwater $\delta^{18}O$ flowing out of an epikarst store, which is balanced by rainfall, evaporation, and dripwater. Water portions in dripwater depends on water ages (described by a time-variant probability distribution, here we use a gamma distribution)
Karstolution	Precipitation $\delta^{18}O$ Precipitation amount Evapotranspiration	Sizes of water stores in soil (soilstore), epikarst (epikarst) and karst (ks1) Flux rates among water stores (f_i) Epikarst evaporation (k_eevap, k_d18o_epi) Other parameters (https://github.com/swasc/karstolution)	Calculating dripwater $\delta^{18}O$ flowing out of a karst water store, with diffuse and conduit inflow from rainfall, soil store, and epikarst

principle, τ can be estimated through tracer dispersion experiments in the karst (McGuire and McDonnell, 2006), but in practice, we can also compare the simulations with different τ values to the cave monitoring data and then select τ of the best-fit simulation. This is realistic because τ and the Peclet number are the only free parameters in this model. The advection-dispersion model is controlled by both residence time and the Peclet number (i.e., the ratio between advection and diffusion of water). A larger Peclet number means that advective transport is more dominant than diffusive transport in fluids. Note that the advective transport is always represented in the advection-dispersion model, but not represented in the well-mixed model. Thus, the Peclet number controls the relative importance of advection vs. diffusion transport in the advection-dispersion model.

3. **SAS** (Harman, 2015). The third approach simulates dripwater $\delta^{18}O$ values as a mixture of recharge precipitation $\delta^{18}O$ values, weighted by their (modeled) prevalence in the epikarst storage and a non-uniform, time-varying storage age selection (SAS) function, following Harman (2015). That is, the model simulates water that is discharged at a drip site as a mixture of water with young and old storage ages. The model also varies the proportion of young vs. old water through time, as related to the amount of storage in the hydrologic system. This approach recognizes that connectivity of flow paths and the tendency for water to use conduit vs. diffuse flow paths can change with antecedent moisture conditions and rainfall amount. The model does not physically simulate flowpaths in the karst system. Instead, it is based on finding a probability distribution Ω_Q (called the "SAS function") that describes how drip water is 'selected' from water of different ages in storage. The distribution of water ages in storage is captured in the age-ranked storage $S_T(T,t)$ (volume of water in the epikarst with an age less than T at time t) whose evolution over time is governed by the conservation of mass for water less than an age T:

$$\frac{dS_T(T,t)}{dt} = J(t) - Q(t)\Omega_Q(S_T,t) - E(t)\Omega_E(S_T,t) - \frac{dS_T(T,t)}{dT} \tag{2}$$

The oxygen isotope ratio $\delta^{18}O$ in dripwater (R_Q) and evapotranspiration (R_E) is the weighted average of water in storage that arrived in the past from precipitation $\delta^{18}O$ (R_J):

$$R_Q(t) = \int_0^1 R_J\left(t - T_{\Omega_Q^*}\right) d\Omega_Q^* \tag{3}$$

$$R_E(t) = \int_0^1 R_J\left(t - T_{\Omega_E^*}\right) d\Omega_E^* \tag{4}$$

here J is the rainfall rate, Q is the drip rate (expressed as volume per time per effective recharge area), E is evapotranspiration rate, and T_{Ω^*} is the age that satisfies $\Omega^* = \Omega(S_T(T_{\Omega^*},t),t)$. Fractionation due to evapotranspiration is not considered here, so the $\delta^{18}O$ value associated with ET is the same as the water store.

The portions of water parcels of different ages are dependent on the assumed probability distribution functions. In this study, we assume the SAS function for the dripwater, Ω_Q, is a gamma distribution, and the distribution is time-variant. That is, the cumulative distribution function of age-ranked storage S_T is defined by Ω_Q:

$$\Omega_Q(S_T,t) = \Gamma(S_T;\alpha,S_Q) \tag{5}$$

$$S_Q = S_o + \Delta S \cdot \lambda \tag{6}$$

where Γ is the incomplete gamma function, α is the shape parameter, and S_Q is the scale parameter. The mean of the distribution is αS_Q, the value of which is indicative of the volume of water turning over in the epikarst as precipitation makes its way to become dripwater. We assume that the shape parameter (which controls how skewed the distribution is) is fixed, but the scale parameter S_Q varies linearly with the variation of ΔS around its mean value S_o (a behavior consistent with previous catchment-scale studies). S_o is an unknown parameter that must be tuned, and ΔS is calculated by tracking the epikarst water balance. The dimensionless parameter λ determines how fast S_Q responds to storage changes. Values of $\lambda < 1$ suggest flow paths transmitting younger water become more efficient under wetter conditions, while $\lambda > 1$ suggests older water become more mobile under wetter conditions. In addition, the SAS function for evapotranspiration (ET) from the epikarst must be specified, since it also affects the age structure of stored water. However, fractionation due to evaporation in soil and epikarst is not considered in SAS. Here the ET SAS function was assumed to be a uniform distribution over the youngest E_0 mm of storage, reflecting root water uptake from surface soils. We assume E_0 = 500 mm, which is similar to the values found in previous studies (Harman, 2015; Wilusz et al.,

2017). In this study, we acknowledge that the parameters we use are not precisely optimized to get the minimum of RMSEs. Rather, a range of values of α, S_0, and λ were explored. We manually explored multiple parameter spaces for each cave dripwater site to find combinations that minimized RMSEs (please see details in Table S2) and at the same time explored the physical meaning of each parameter. The parameters include the (temporal) mean water storage size S_0, depth of root water uptake E_0, and two parameters controlling the shape (α) and scale sensitivity to epikarst storage (λ) of the dripwater SAS function.

4. **Karstolution** (Treble et al., 2019). The fourth approach employs several reservoirs representing the soil, epikarst, and vadose zone, along with monthly climate inputs, to simulate stalagmite growth and geochemistry (Treble et al., 2019). The model comprises two parts, to represent karst processes and in-cave processes. Karstolution couples previous stalagmite and karst-based forward models KarstFor (Baker and Bradley, 2010; Treble et al., 2013) and ISOLUTION (Deininger et al., 2012). The former simulates karst processes and the latter simulates in-cave geochemical processes. The karst processes include oxygen isotope fractionation during evaporation, mixing amongst water from matrix flow and conduit flow from water stores, and overflow movement (water flows out of a water store when the water level in this store exceeds a threshold). The model simulates various water pathways through soil water store, epikarst store, and two underlying water stores before surface precipitation reaches the cave ceiling. The model generates five different types of stalagmites with different weights of their water sources (e.g., water store, matrix flow, and overflow). Thus, the model has multiple additional parameters that require constraints compared to the previous three models evaluated in this study. The Karstolution parameters used in this study are listed in Table S3. Since Karstolution physically simulates flow pathways and water stores, exploring its parameters provides opportunities to learn and test hypotheses surrounding cave/karst processes.

By evaluating this suite of modeling approaches, we employ a tiered-analysis focusing on differences in complexity (Table 1). PRYSM, SAS, and Karstolution models were executed using Python scripts freely available via https://github.com/sylvia-dee/PRYSM, https://github.com/charman2/mesas, and https://github.com/swasc/karstolution, respectively. SAS was run using a daily time step, while other models were run using a monthly time step.

3. Results

3.1. Texas caves

3.1.1. Cave dripwater $\delta^{18}O$

Variability in cave dripwater $\delta^{18}O$ values is muted relative to variability in precipitation $\delta^{18}O$ values (Fig. 1a). This muted variability is consistent with existing cave monitoring studies at this site (Pape et al., 2010; Feng et al., 2014) and other locations around the world (Cruz et al., 2005; Lambert and Aharon, 2011; Partin et al., 2012; Oster et al., 2012). Mean $\delta^{18}O$ values at three of the four drip sites are consistent with the long-term amount-weighted mean precipitation $\delta^{18}O$ value (−4.3‰), whereas one site (NBBC) has a larger average $\delta^{18}O$ value (−3.8‰; Fig. 2). Cave dripwater $\delta^{18}O$ values appear insensitive to large, inter-annual fluctuations of moisture conditions above the cave (e.g., floods and droughts) and tend to dramatically smooth the input climate signal on sub-annual time scales (Fig. 1a). Only the drought during 2008–2010 and the flood during 2010–2011, were preserved in cave dripwater $\delta^{18}O$ of

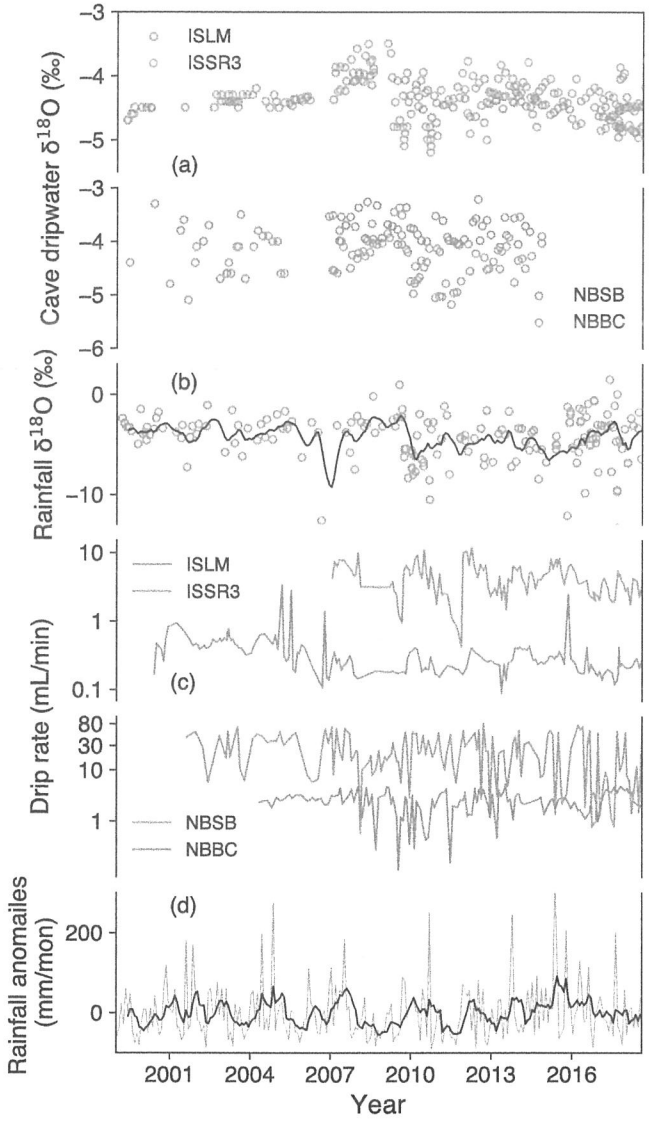

Fig. 1. Time series of precipitation and cave dripwater $\delta^{18}O$ variability in Texas. (a) Cave dripwater $\delta^{18}O$ of four drip sites ISLM (green circles), ISSR3 (orange circles), NBSB (purple circles), and NBBC (pink circles) in Natural Bridge Caverns (NB) and Inner Space Cavern (IS). (b) Rainfall $\delta^{18}O$ (gray circles) at the campus of the University of Texas, Austin (UT) with the 12-month (unweighted) running mean of its rainfall $\delta^{18}O$ values (black curve, monthly data). (c) Drip rates of four drip sites ISLM (green line), ISSR3 (orange line), NBSB (purple line), and NBBC (pink line). (d) Monthly rainfall anomalies (gray line) at UT with its 12-month running mean (black line). Rainfall anomalies are calculated by the monthly rainfall amount subtracting its climatological mean. (For interpretation of the references to colour in this figure legend, the reader is referred to the Web version of this article.)

conduit flow sites ISSR3 and NBSB (Fig. 1a, d). Cave dripwater $\delta^{18}O$ variation is typically less than 2‰, whereas when moisture conditions fluctuate between drought and flooding, precipitation $\delta^{18}O$ values span a 10‰ range. This indicates that cave dripwater $\delta^{18}O$ and probably speleothem $\delta^{18}O$ in these caves does not register most of interannual variability of droughts and floods (Pape et al., 2010). In addition, it should be noted that cave drip rates are more sensitive to different hydroclimate episodes than dripwater $\delta^{18}O$ (Fig. 1c, d). This implies reconstructions from the region's speleothem $\delta^{18}O$ may be best suited for reflecting longer-term changes (e.g., decadal changes) in rainfall, while studies with the goal of reconstruction of shorter-term variability may best be done at

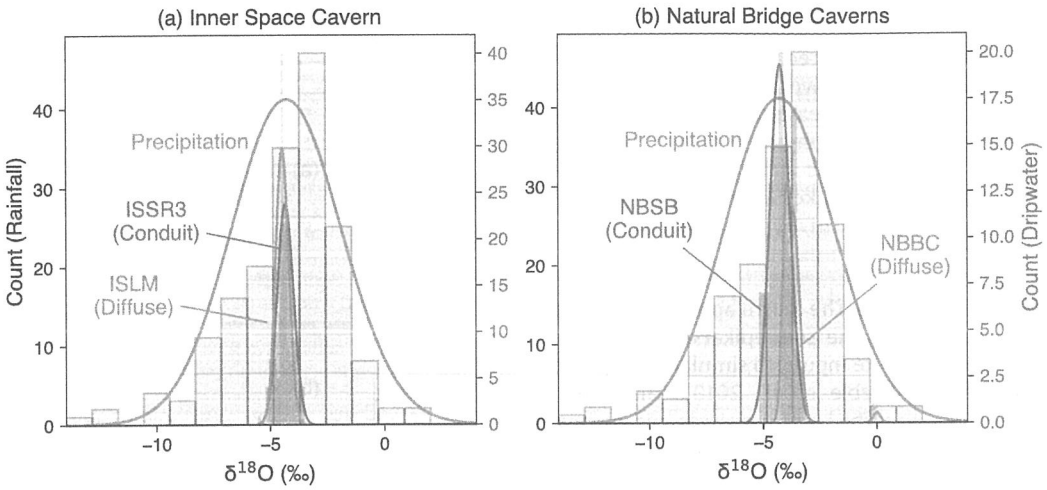

Fig. 2. Histograms of precipitation and cave dripwater $\delta^{18}O$ values highlight the limited variability in cave dripwater relative to precipitation $\delta^{18}O$ values. Colored lines are estimated kernel density functions of precipitation (green lines) and cave dripwater $\delta^{18}O$ (red and blue lines). The conduit-type drip sites ISSR3 (standard deviation (SD) = 0.35) and NBSB (SD = 0.43) have higher standard deviations of dripwater $\delta^{18}O$ than their diffuse-type counterparts ISLM (SD = 0.28) and NBBC (SD = 0.24), respectively. (For interpretation of the references to colour in this figure legend, the reader is referred to the Web version of this article.)

conduit-dominated drip sites.

The histograms of precipitation and cave dripwater $\delta^{18}O$ (Fig. 2) also show that cave dripwater $\delta^{18}O$ is characterized by a much lower variance than precipitation $\delta^{18}O$. In both IS and NB caves, the conduit-type dripwater $\delta^{18}O$ has a larger variance than the diffuse-type. In IS caves, the median of precipitation $\delta^{18}O$ and dripwater $\delta^{18}O$ at two sites are comparable (−4.5‰ and −4.3‰), but in NB caves, the median of diffuse-type dripwater $\delta^{18}O$ (NBBC: −3.8‰) is more positive than the median of precipitation and conduit-type dripwater $\delta^{18}O$ (NBSB: −4.2‰). This difference is likely due to the fractionation of evaporation in epikarst, a conclusion supported by the simulation of Karstolution (see Section 3.1.2).

3.1.2. *Proxy system model inter-comparison*

Four PSMs of varying complexity were applied to simulate cave dripwater $\delta^{18}O$ time series at several different drip sites, which were then compared directly with the above-described cave monitoring data (Fig. 3).

For the simulations of the RM model, we tested two cases, one using a 12-month average and another using a 24-month average; these values were chosen due to the fact that previous studies (Wong et al., 2011; Bunnel, 2019) estimated the residence time of dripwater of these two caves as 1–2 years. Since the rainfall amount and precipitation $\delta^{18}O$ data used here are the same for the four cave dripwater sites in Texas (we use precipitation $\delta^{18}O$ data at the campus of UT Austin to represent precipitation $\delta^{18}O$ in all caves, Methods), all of the simulated dripwater $\delta^{18}O$ time series shown in Fig. 3A are the same. Using the RM method, the simulated cave dripwater $\delta^{18}O$ has larger variance (ranging from −7 to −3‰) than the monitoring data (−5 to −3.5‰); the 12-month average model features larger variance than the 24-month average model, which is to be expected given that averaging over longer time decreases the variance of the time series.

In PRYSM simulations, we tested both cases with residence times of 12 and 24 months, respectively (consistent with the parameter selection in the RM simulations), and set the Peclet number to 1 (i.e., in the advection-dispersion model, advective transport is equally important as diffusive transport.) (Fig. 3B). The variability in the simulated cave dripwater $\delta^{18}O$ is lower than that produced by the RM model. PRYSM successfully simulates the correct amplitudes of major $\delta^{18}O$ excursions, such as positive anomalies in 2008 at ISLM, ISSR3, and NBSB, and negative anomalies in 2011 at ISLM, ISSR3, and NBSB. However, the simulated cave dripwater $\delta^{18}O$ for NBBC deviates the mean of the observations by about 1‰. As expected, the simulations with longer residence times have smaller variance (Fig. 3B) because more old water mixes with young water, which dampens the dripwater $\delta^{18}O$ variability. Moreover, the simulations produced by the well-mixed model exhibit smaller $\delta^{18}O$ variance compared to the advection-dispersion model (Figs. 3B and 6B), confirming that the explicit simulation of advection facilitates faster water flows, resulting in quicker responses to rainfall $\delta^{18}O$.

The simulations of the SAS model are shown in Fig. 3C. Even without precise calibrations (i.e., optimizing the model with one set of parameters), the SAS model simulates a strong fit to the monitoring data. SAS not only reproduces the range contained in the observations (~ 1‰ at caves ISLM, ISSR3, and NBBC, and ~ 2‰ at cave NBSB, Fig. 3C), but also accurately simulates major excursions of cave dripwater $\delta^{18}O$, especially for ISLM and NBSB (see, for example, years 2007, 2009, and 2011, Fig. 3C). Small α values make the distribution of dripwater age skewed – both very old and young water have larger proportions, so the simulations with small α values feature large variance (ISLM and ISSR3 in Figs. 3C and 6C). Large λ values indicate that more older water (i.e., the more well-mixed water) comprises the outflow/dripwater, such that simulations with large λ values show lower variance (NBSB in Figs. 3C and 6C).

Finally, the simulations of the more complex process-based speleothem model, Karstolution, are shown in Fig. 3D. We explore the impacts of several parameters on the dripwater $\delta^{18}O$ in Fig. 3D. Setting lower values of the flow from soil store to epikarst (f1), soil store size (soilstore), drainage flux of the main karst water store (f5), and larger main karst water store size (ks1) extends the storage of water in various stores, which in turn extends the residence time of water in the karst system. These processes result in lower variability of the simulated cave dripwater $\delta^{18}O$ in ISLM and NBSB, providing a better match to the monitoring data (blue lines in Fig. 3D). Furthermore, setting higher values of the isotopic evaporation coefficient for epikarst store (k_d18O_epi) and the fraction of water in epikarst available to evaporate (k_eevap) in ISSR3 and

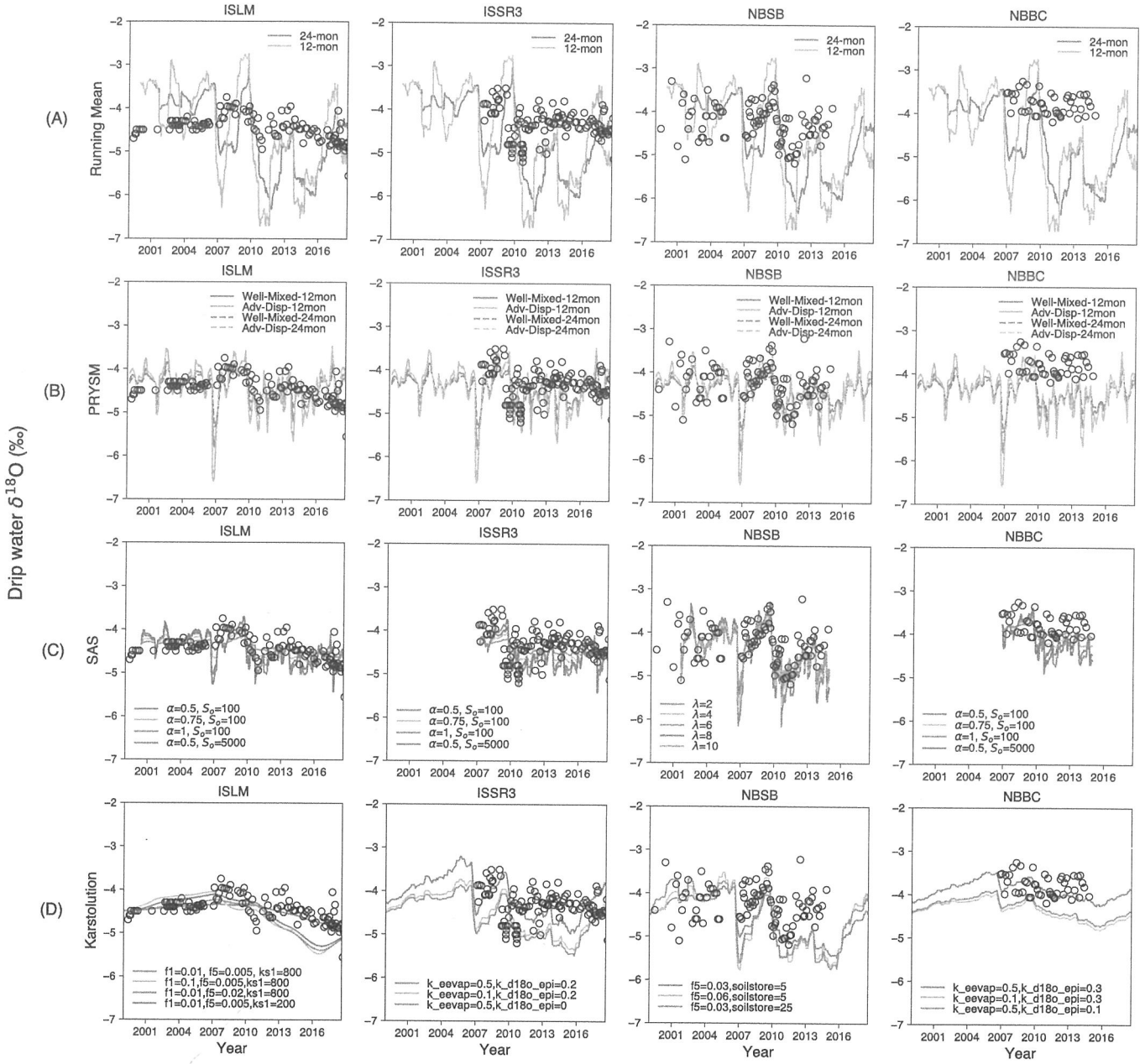

Fig. 3. Comparison of simulated (lines) and observed Texas cave dripwater $\delta^{18}O$ (black circles) variability for the different modeling approaches. (A) The 12- (blue) and 24-month (orange) amount-weighted running mean precipitation $\delta^{18}O$ are shown in the top row. (B) PRYSM modeling using tau-values from 10 to 20 months are shown in the second row for the well-mixed (blue) and advection-dispersion model (orange; Peclet number of 1 for all simulations). (C) The SAS model (third row) was parameterized for NBSB using $\alpha = 0.5$, $S_o = 500$, and $E_o = 500$, and λ values from 2 (blue) to 10 (magenta). For ISLM, ISSR3, and for NBBC sites, SAS was parameterized using $\lambda = 10$, $S_o = 100$, and $E_o = 500$, and α values of 0.5 (blue), 0.75 (orange), and 1.0 (green), and, for comparison, $\lambda = 10$, $\alpha = 0.5$, $S_o = 5{,}000$, and $E_o = 500$ (red). (D) Karstolution model (bottom row) was parameterized for ISLM using f1 = 0.01, f5 = 0.005, ks1 = 800 (blue) and then f1 set to 0.1 (orange), f5 set to 0.02 (green), and ks1 set to 200 (red). For ISSR3, Karstolution was parameterized using k_eevap = 0.5 and k_d18o_epi = 0.2 (blue) and then k_eevap set to 0.1 (orange) and k_d18o_epi set to 0 (green). For NBSB, f5 was set to 0.03 and soilstore = 5 (blue) and then f5 set to 0.06 (orange) and soilstore set to 25 (green). For NBBC, k_eevap = 0.5 and k_d18o_epi = 0.3 (blue) and then k_eevap set to 0.1 and k_d18o_epi set to 0.1. The detailed parameterization is in Table S3. (For interpretation of the references to colour in this figure legend, the reader is referred to the Web version of this article.)

NBBC (blue lines in Fig. 3D) results in a more accurate simulation of cave dripwater $\delta^{18}O$ in these two sites, especially considering the high $\delta^{18}O$ values observed at NBBC. This indicates that evaporation in epikarst plays an important role in determining cave dripwater $\delta^{18}O$ of ISSR3 and NBBC. Moreover, the simulated cave dripwater $\delta^{18}O$ of ISSR3 and NBBC successfully captures the flood/drought tranistions in 2007 and 2010 when comparing with rainfall amount above caves (Fig. 1d).

To better quantify the performance of each model, we calculated the root mean square errors (RMSEs) for each modeled cave dripwater $\delta^{18}O$ time series. The result is synthesized in Fig. 4. The RM model has the largest RMSEs for all simulations, while the RMSEs of SAS and Karstolution are comparable (0.2–0.6‰ for all drip sites except NBBC). RMSEs for PRYSM are the smallest (0.01–0.25‰) except for NBBC. The NBBC site is challenging for all models because of its exceptionally high isotope ratios measured in the mean cave dripwater $\delta^{18}O$. This suggests that PRYSM, SAS, and Karstolution can adequately simulate cave dripwater $\delta^{18}O$. While PRYSM

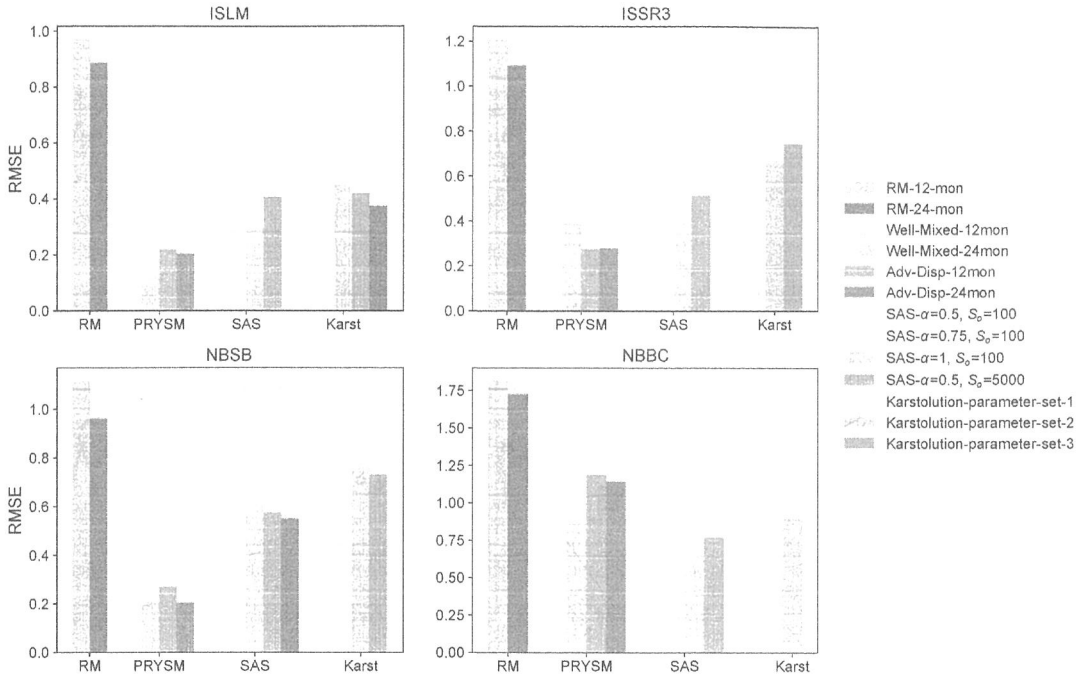

Fig. 4. Comparison of root mean square errors of modeled cave dripwater $\delta^{18}O$ shown in Fig. 3. These models and parameter sets are: the RM model (blue bars) with 12-month average and 24-month average, PRYSM model (green bars) with the well-mixed mode and advection-dispersion mode. The parameterization settings for the SAS model (orange bars) and Karstolution model (purple) are the same as Fig. 3. The detailed parameter settings for SAS and Karstolution are listed in Table S2 and S3. (For interpretation of the references to colour in this figure legend, the reader is referred to the Web version of this article.)

provides some advantages compared to SAS and Karstolution, with fewer inputs and parameter settings, the more complex models provide more refined simulations of karst processes (e.g., flow pathways, water store size, evaporation in epikarst). Thus, simulations derived from both SAS and Karstolution provide opportunities for thorough investigations of site-specific karst processes, for example.

3.2. Borneo caves – A tropical complement

As a complementary analysis in a contrasting climate, we simulated cave dripwater $\delta^{18}O$ for Borneo caves, as originally published in Moerman et al. (2014) and Ellis et al. (2020). The results suggest that all four models, including the RM model, simulate Borneo dripwater $\delta^{18}O$ well, especially for drip sites WF and WS (Fig. 5). The average RMSEs of these simulations are all less than 0.2‰, substantially out-performing the simulations of Texas cave dripwater, whose average RMSEs are approximately 0.3–1.7‰. This difference is largely due to the short residence time of dripwater in Borneo caves, which is estimated to be 3 months (Moerman et al., 2014), compared to 12–24 months for the sites studied in Texas caves. The relatively short residence time makes the cave dripwater $\delta^{18}O$ much more responsive to precipitation $\delta^{18}O$ changes on shorter time scales. A shorter residence time also serves to limit the contributions of complicating karst processes, such as mixing, before cave drip and calcification. There are notable offsets between dripwater $\delta^{18}O$ of Lang's cave (L2) and its simulations from RM and PRYSM. Moerman et al. (2014) used a two-box mixing model (one with the residence time of 10 months and another with invariant water $\delta^{18}O$) to simulate L2. Our simulation by SAS shows that increasing the epikarst store size (changing S_0 from 500 to 3600 mm) can also resolve the model-data discrepancy (Fig. 5C). In addition, in Karstolution, decreasing the drainage flux rate of the karst water store achieves a similar result (Fig. 5D). Taken together, these simulation results indicate the drip site L2 either has a larger water store size, or an exceptionally slower drainage flux rate of the water store source than WF and WS.

4. Discussion

4.1. Texas caves

The simplified PSM which employs a running mean (RM model) does not adequately simulate cave dripwater $\delta^{18}O$ measured *in-situ* in four Texas cave drip sites. The RM model overestimates the variability of observed $\delta^{18}O$ values, though it simulates the mean values correctly. However, all of the intermediate-to-comprehensive models (PRYSM, SAS, and Karstolution) simulate cave dripwater $\delta^{18}O$ well (RMSEs are within 0.3‰ of the analytical error range, except for NBBC), and capture the variance of observed/measured $\delta^{18}O$ (Fig. 6) and the amplitudes of several major isotope excursions (e.g., positive anomalies in 2008 at ISLM, ISSR3, and NBSB, and negative anomalies in 2011 at ISLM, ISSR3, and NBSB. See Fig. 3 for reference).

Since PRYSM requires fewer parameters to be tuned than SAS and Karstolution, PRYSM may prove practical for simulating cave dripwater and speleothem $\delta^{18}O$ over a network of sites where the karst information is poorly constrained or inconsistent amongst sites. For example, PRYSM could be used to simulate a network of caves in similar subtropical climates. However, if site-specific hydrology is known, SAS and Karstolution provide robust simulations compared to observations for the four drip sites, and minimize the model-data RMSE in all cases. SAS and Karstolution are thus particularly useful for site-specific constraints or in-situ data-model comparisons focused on local hydrology. Moreover, Karstolution physically simulates flow pathways and water stores; its parameters have intuitive physical meaning, facilitating investigations of cave processes including water store sizes, flow rates between water stores, and epikarst evaporation. The model's parameters allow the user to partition the impacts of these various

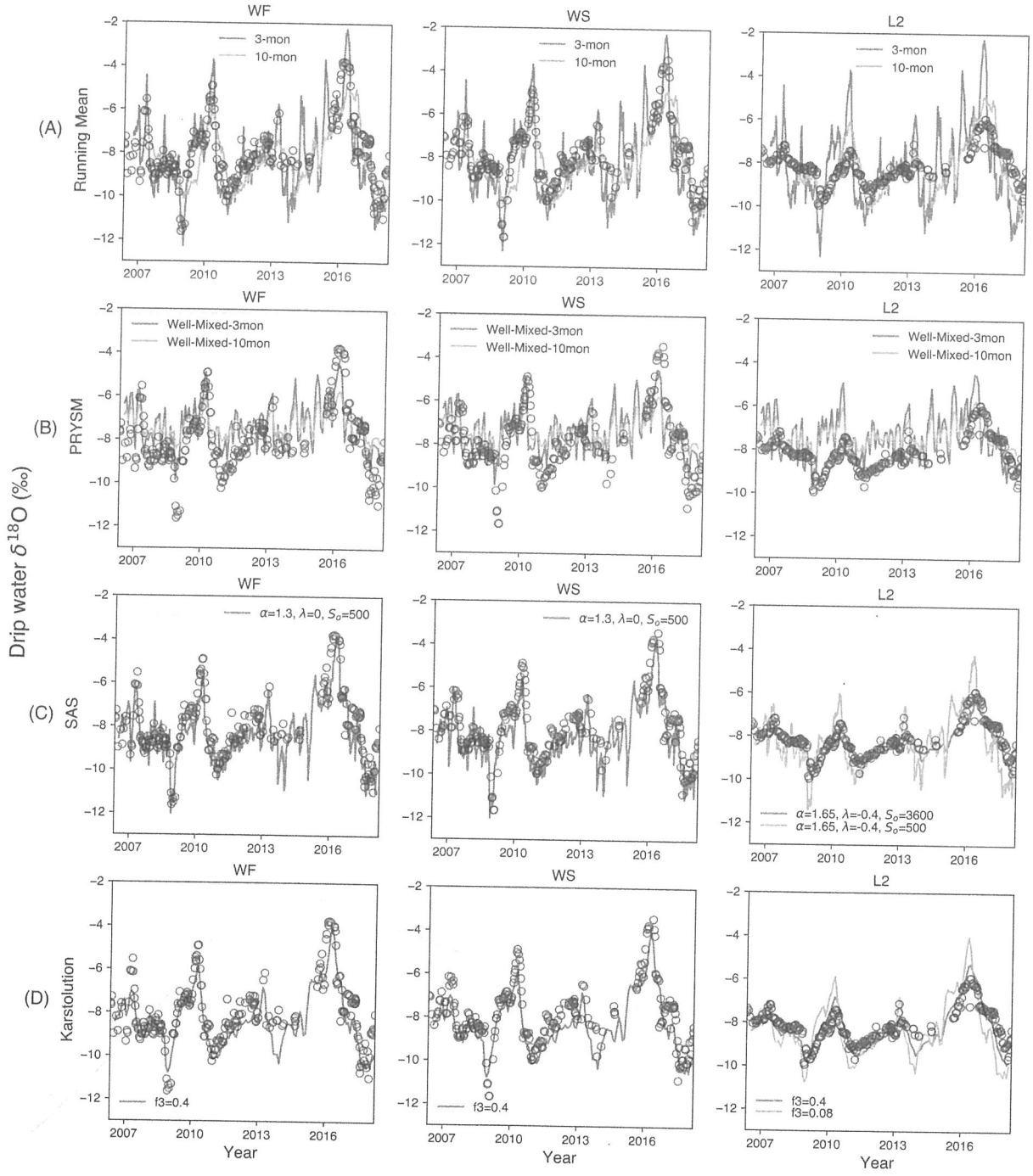

Fig. 5. Comparison of simulated (curves) and observed (circles) Borneo cave dripwater $\delta^{18}O$ variability for the different modeling approaches. The 3-month (blue) and 10-month (orange) amount-weighted running mean precipitation $\delta^{18}O$ are shown (A). PRYSM modeling (B) using tau-values of 3 months (blue) and 10 months (orange) are shown for the well-mixed model. The SAS model (C) was parameterized using $\alpha = 1.3$, $S_o = 500$, $E_o = 1500$, and $\lambda = 0$ for WF and WS. SAS was parameterized with $\alpha = 1.65$, $S_o = 3600$ (blue)/ $S_o = 500$ (orange), $E_o = 3200$, and $\lambda = -0.4$ for L2. The Karstolution model (D) was parameterized using f3 = 0.4 for WF and WS; f3 was set for 0.4 (blue) and 0.08 (orange) for L2. Please see other parameters in Karstolution in Table S3. (For interpretation of the references to colour in this figure legend, the reader is referred to the Web version of this article.)

processes. For example, by exploring the parameters controlling evaporation fractionation in epikarst (Fig. 3D), we conclude that epikarst evaporation cannot be ignored for sites ISSR3 and NBBC, especially for explaining the higher mean values of dripwater $\delta^{18}O$ in NBBC.

To constrain the individual impacts of various model parameters on the simulated dripwater $\delta^{18}O$, a suite of probability distribution functions of dripwater $\delta^{18}O$ for different sets of parameters are given in Fig. 6. These parameter sets are selected from Fig. 3 and their RMSEs are shown in Fig. 4. The RM model (Fig. 6A) simulates a larger spread in $\delta^{18}O$ than the observations, while a longer running mean window (24 months) decreases the variance of simulated dripwater $\delta^{18}O$. For PRYSM (Fig. 6B), the variance of the well-mixed model is closer to the observed dripwater $\delta^{18}O$ in the "diffuse" cave drip site ISLM, while the variance of the advection-dispersion model provides a closer match to observations in the "conduit"

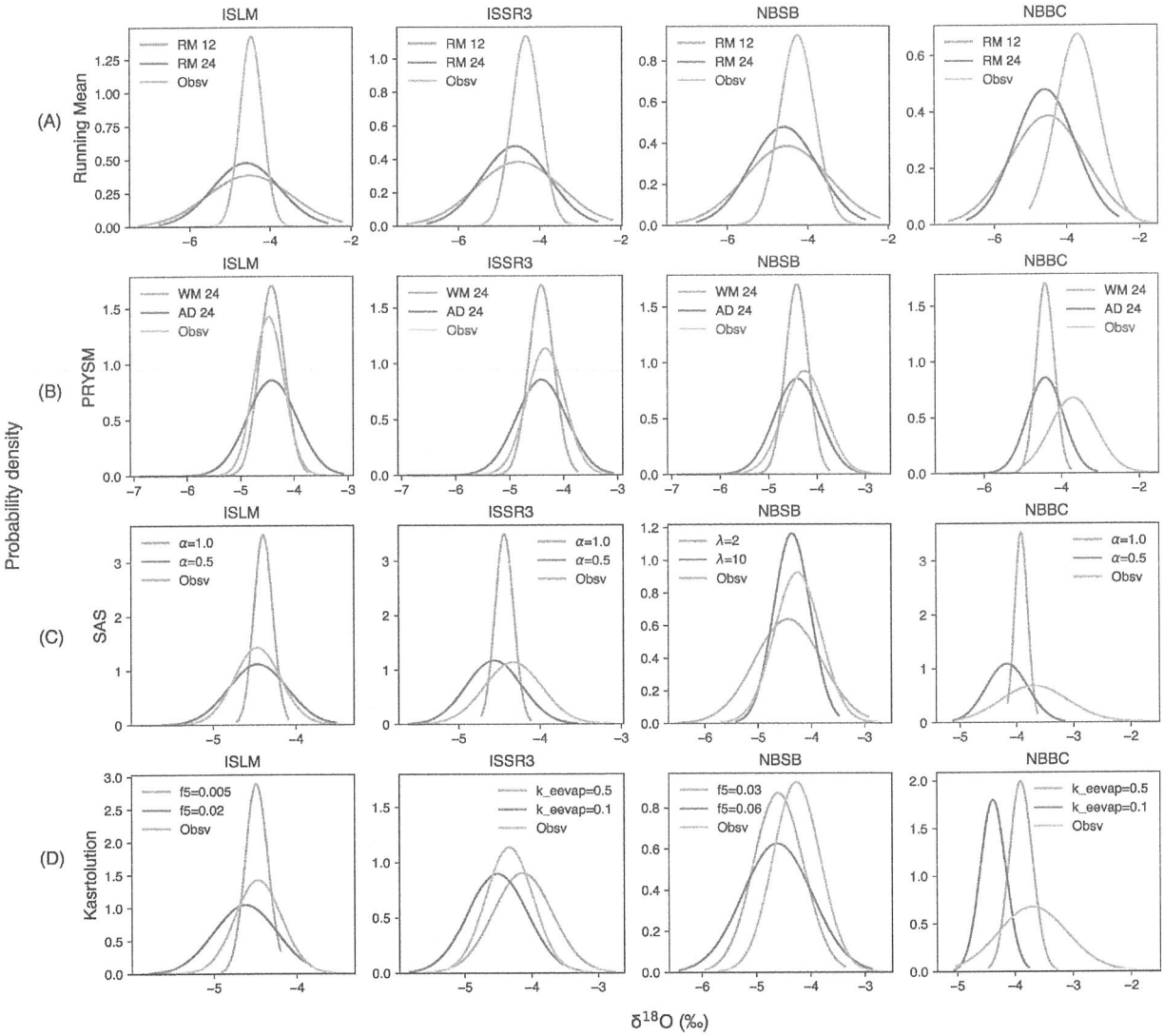

Fig. 6. Comparison of probability distribution functions (PDFs) of modeled (red and blue) and observed (green) cave dripwater $\delta^{18}O$ values selected from Fig. 3. PDFs are shown for 12-month (red) and 24-month (blue) amount-weighted running mean precipitation $\delta^{18}O$ (A), modeled dripwater $\delta^{18}O$ by the well-mixed (τ = 20 months; WM 20, red) and advection-dispersion (τ = 10 months; AD 10, blue) mode in PRYSM (B), modeled dripwater $\delta^{18}O$ by SAS (C), α = 1 (red) and α = 0.5 (blue) for ISLM, ISSR3, and NBBC caves; λ = 2 (red) and λ = 10 (blue) for NBSB cave, and modeled dripwater $\delta^{18}O$ by Karstolution (D), k_eevap = 0.5 (red) and k_eevap = 0.1 (blue) for ISSR3 and NBSB; f5 = 0.005 (red) and f5 = 0.02 (blue) for ISLM; f5 = 0.03 (red) and f5 = 0.06 (blue) for NBSB. (For interpretation of the references to colour in this figure legend, the reader is referred to the Web version of this article.)

cave drip sites. This suggests that the well-mixed model in PRYSM may be more suitable for diffuse drip sites, while the advection-dispersion model is more suitable for the conduit drip sites, matching our physical understanding of how these models represent flow paths and mixing. For SAS (Fig. 6C), the shape parameter α describing the probability function of age ranks in groundwater has large impacts on the variance of dripwater $\delta^{18}O$: setting it to 0.5 instead of 1.0 results in a more highly skewed dripwater age distribution, with a larger proportion of very young water, but also larger contributions of very old water. This produces a better fit with the variance of observations. In addition, the parameter λ controlling the size of water storage strongly influences the variance of dripwater $\delta^{18}O$. Larger λ, indicating more mobilization of older water under wet conditions, provides the closest model fit to the NBSB record. For Karstolution (Fig. 6D), larger drainage flux (f5) increases the variance of dripwater $\delta^{18}O$ (ISLM and NBSB), and a larger fraction of epikarst water available for evaporation fractionation (k_eevap) makes dripwater $\delta^{18}O$ more positive (ISSR3 and NBBC). This result indicates the importance of considering fractionation during evaporation of epikarst in Texas caves.

This work underscores the importance of considering differences between conduit-type drip sites and diffuse-type drip sites in the choice of a PSM. Dripwater $\delta^{18}O$ of conduit-type sites has larger variance than diffuse-type sites. This is expected as conduit-type sites are more connected to the surface, so they are more responsive to rain events and thus contain larger signal variance (Wong et al., 2011). The PRYSM simulation shows that its well-mixed mode is more suitable for diffuse-type sites and the advection-dispersion mode is more suitable for conduit-type sites (Fig. 6B). The differences between the two modes is due to the response functions in PRYSM. The advection-dispersion mode has a shorter but stronger response to rainfall events than the well-mixed mode, and these features essentially capture the differences between conduit-type and diffuse-type sites. The conduit-type sites are characterized by a shorter water residence time, while the diffuse-type sites typically exhibit longer residence times, allowing water

of various ages to mix. Given this functionality of PRYSM, we note that users should employ the well-mixed mode for diffuse-type sites and the advection-dispersion mode for conduit-type sites.

4.2. Borneo caves

The Borneo caves, which are located in a high-precipitation, tropical climate regime, yield inherently different results compared to simulations for Texas caves. All four models, including the RM model, simulate cave dripwater $\delta^{18}O$ with accuracy (Fig. 5). The average RMSEs of these simulations are all less than 0.2‰, substantially out-performing the simulations of Texas cave dripwater. The result implies that the selection of appropriate PSMs depends on the structure of the cave, specifically the residence time of water in the cave system. Drip sites in Borneo caves have shorter residence times and potentially simpler flow pathways. This likely accounts for the success of the simplified model in simulating tropical dripwater $\delta^{18}O$ compared to the drier, subtropical Texas caves in this study. Rainfall may directly diffuse through soil and epikarst and reach the ceiling of Borneo caves with little mixing with water stores of different ages. Site L2 may have more complicated flow pathways than WF and WS, but we can still simulate it by simply adding a mixing reservoir (Moerman et al., 2014).

The climate at the cave site may also have an impact. In tropical humid regions such as Borneo, there is likely little evaporation of water stored in the karst system; in contrast, in arid or sub-arid regions, evaporation of water stores in the karst system drives large changes in dripwater $\delta^{18}O$ via evaporative enrichment of the water isotopes. A more complex model is required to estimate the impacts on the dripwater caused by evaporative and storage/mixing processes, evident from the Karstolution simulations. For a cave in a humid climate with relatively short residence times, a simple running weighted-average model is sufficient to simulate cave dripwater $\delta^{18}O$, and thus, likely sufficient to model the resultant speleothem calcite $\delta^{18}O$. For caves with longer residence times (>6 months) and in sub-arid regions, intermediate complexity models such as PRYSM, SAS, and Karstolution are necessary to simulate cave dripwater $\delta^{18}O$ with fidelity. In addition, Borneo drip sites register interannual hydroclimate variability such as ENSO (Moreman et al., 2014) due to their short residence times, while Texas drip sites may not faithfully record interannual hydroclimate variability. This difference informs the interpretation of speleothem records from different climatic regions.

4.3. Selection of PSMs

All four models discussed in this study have advantages and disadvantages in simulating cave dripwater $\delta^{18}O$ and possibly speleothem $\delta^{18}O$.

The RM model is very convenient to use due to its simplicity and is accurate for drip sites with short residence times (<6 months) and simple flow pathways. RM can simulate dripwater $\delta^{18}O$ at Borneo sites WF and WS. However, the accuracy of RM decreases for caves with long residence times and complex flow pathways, such as the Texas caves studied here. Given the simplicity of RM, it is also useful for estimating residence times which best fit monitoring data by exploring possible ranges of residence times.

PRYSM is also convenient to use, and only requires two parameters – residence time (tau) and Peclet number. It is also easily coupled to GCM outputs, facilitating the translation of climate model simulations to pseudo-stalagmites $\delta^{18}O$. Our results demonstrate that PRYSM simulates dripwater $\delta^{18}O$ in better agreement with available data compared to the RM model, and reduces RMSE compared to more complex, comprehensive models SAS and Karstolution. However, PRYSM falls short in simulating drip sites with complex flow pathways (e.g., simulation of site L2). In addition, PRYSM does not allow the user to explore cave/karst processes and combinations of different flow pathways. Thus, we recommend PRYSM specifically for applications simulating global pseudo-speleothem $\delta^{18}O$ using climate model simulations as inputs.

SAS is a comprehensive model designed for simulating solute transport in hydrodynamic systems. If it can be coupled with a model of in-cave carbonate fractionation like ISOLUTION, SAS can also simulate pseudo-stalagmite $\delta^{18}O$. Based on our evaluation, SAS can simulate cave dripwater $\delta^{18}O$ well after manually tuning the four main parameters listed in Table 1. Thus SAS provides a strong option for simulating local dripwater $\delta^{18}O$. SAS also provides additional information surrounding the transport of different ages of water in the cave, which can be readily constrained using SAS for parameter optimization problems. Moreover, SAS can extend our understanding of the water balance of groundwater (which it requires as input). After tuning its parameters with cave monitoring data, we can use SAS to estimate the volume of water stored in catchments/underground in the past and future that is actively turning over and contributing to drip water recharge.

Karstolution is a comprehensive physics-based model made for simulating stalagmite $\delta^{18}O$. Based on our evaluation, Karstolution can simulate cave dripwater $\delta^{18}O$ if parameters are properly tuned. A key advantage of Karstolution is the ability to constrain cave/karst processes such as flow rates between water stores, sizes of water stores in the karst system, and fractionation due to epikarst evaporation. The model physically simulates mixing/diffusion processes and flow pathways. It can be also employed to test hypotheses on cave/karst processes. For example, we used Karstolution to confirm the importance of epikarst evaporation in drip sites ISSR3 and NBBC. Though there are many site-specific parameters required to run Karstolution simulations, it is useful for cave-specific hydrology studies.

4.4. Choices of parameters in PSMs

Both RM and PRYSM require an estimation of the water residence time in karst systems, which cannot be directly measured via cave monitoring. Though in principle, residence time can be estimated through tracer dispersion experiments in the karst (McGuire and McDonnell, 2006), we can also estimate it based on the geometry of the cave, porosity, and drip rates. Partin et al. (2012) gave an example of quickly estimating the residence time (τ):

$$\tau = \frac{V\varphi}{\left(S/d^2\right)\cdot F} \tag{7}$$

where V is the bedrock volume, which can be estimated by the cave depth and the size of the cave cone, φ is the porosity of the above soil and epikarst, S is the area of the cave ceiling, d is the average distance between drips on the ceiling, and F is the average drip rate of drip sites. We can apply this estimated residence time to the RM model and iterate to find the best fit. Indeed, the RM model itself is a tool to determine the residence time (e.g. Ellis et al. (2020)).

There are four main parameters (listed in Table 1) to tune for running SAS. We suggest tunning the parameters one by one based on our understanding of each parameter instead of tunning all parameters together. For example, as shown above, adjusting to larger λ values reduces the variance of dripwater $\delta^{18}O$. If further optimization of parameters is needed, the DiffeRential Evolution Adaptive Metropolis (DREAM) algorithm (Vrugt, 2016) can be applied to find the parameter set for the best fit model following

Wilusz et al. (2017).

Karstolution is best run by adjusting parameters one by one based on local physical understanding for each parameter. For example, as shown above, setting low values of drainage flux of the karst water store (f5) decreases the variance of dripwater $\delta^{18}O$; a high fraction of epikarst water available for evaporation (k_eevap) makes the mean of dripwater $\delta^{18}O$ more positive. Tuning these parameters is also an opportunity to better understand the cave/karst processes in the study drip site.

4.5. Caveats and future perspectives

We note important caveats of this work: we are evaluating how PSMs simulate cave dripwater $\delta^{18}O$ instead of speleothem $\delta^{18}O$, so future work is needed to evaluate the capability of models in simulating in-cave processes such as equilibrium and kinetic fractionation during the formation of speleothems. Secondly, the analysis presented here using four unique models underscores the fact that it is still challenging to simulate cave dripwater $\delta^{18}O$ in sub-arid and arid climates. Future investigations are needed to study how these PSMs perform in different climate regimes, beyond the two regimes examined here. Furthermore, it should be noted that the parameters of these PSMs have not been fully optimized to minimize RMSEs. We explored different sets of parameters to explore the sensitivity of simulated dripwater to these parameters, but future work is needed to constrain optimal parameters for each model.

In addition, there are other karst/speleothem models not discussed in this study. For example, global karst hydrology models such as VarKarst-R (Hartmann et al., 2015) simulate large-scale karstic groundwater recharge and incorporate karst processes (Baker et al., 2019). These models can be coupled to climate models and modified to simulate global cave dripwater and speleothem $\delta^{18}O$. Similar to Karstolution, model KarstMod (Mazzilli et al., 2019) can also physically simulate karst discharge and be used to analyze cave/karst processes. Since this study focuses on evaluating models against monitored dripwater $\delta^{18}O$, in-cave carbonate fractionation is not discussed herein.

In terms of observations, rainfall amount and rainfall $\delta^{18}O$ were monitored only at one site (Austin) to represent all cave sites in Texas, due to limitations associated with conducting continuous monitoring at multiple sites. This likely imparts some systematic bias in our results, although rainfall amount data at each site is highly correlated to rainfall at the Austin site (Please see the Methods section for the correlations). The observational daily evapotranspiration data is also not monitored in-situ; thus, we extracted a regional average from a reanalysis data set. Finally, the significantly different characteristics of cave dripwater $\delta^{18}O$ in the two close caves in Texas explored in this work underscores the importance of cave monitoring in interpreting speleothem records. We suggest expanding the monitoring of in-situ rainfall and evaporation when designing cave monitoring in arid and semi-arid climates (although this is clearly challenging to achieve, especially for the monitoring of evaporation). For example, automated evaporation pans are costly compared to plain evaporation pans. Expanding cave monitoring and speleothem model evaluations for cave systems in dry climates would enable progress toward, for example, identifying missing physical processes in speleothem models and improve their performance.

4.6. Implications for paleoclimate studies

The cave dripwater $\delta^{18}O$ data from Texas suggests that interannual-scale hydroclimate events, including droughts and floods, may not be preserved in all regional dripwaters, nor in speleothem $\delta^{18}O$ (Pape et al., 2010; Feng et al., 2014; Hulewicz, 2015; Baker et al., 2019; Bunnell 2019). The interannual variability in precipitation is largely smoothed out by groundwater mixing and cave processes; only droughts and floods lasting for several years imprint on the cave dripwater $\delta^{18}O$ (though we acknowledge this time series is short compared to the timescale of the speleothem hydroclimate record). This indicates that speleothem $\delta^{18}O$ in subtropical regions, prone to drought conditions and variable hydroclimate, may only register long-term (i.e. decadal) hydroclimate shifts, and may not be suitable for investigating drought variability at interannual time scales. This conclusion is limited to this set of drip sites and should be tested for more drip sites in both karst systems (Inner Space Cavern and Natural Bridge Caverns) and other karst systems in subtropical regions.

5. Conclusions

Speleothem oxygen-isotope values are widely used to constrain past low-frequency variability in the hydrological cycle. To better understand speleothem records, speleothem PSMs directly transfer climate variables to speleothem $\delta^{18}O$, giving us quantitative frameworks for comparing paleoclimate data to climate model outputs. However, the proper use of speleothem PSMs requires a verification of their reliability and usefulness for a variety of scientific questions.

To this end, the paper aims to evaluate which speleothem PSMs are most suitable for simulating speleothem records in different climate regimes. Long term monitoring data (19-year cave dripwater data sets from semi-arid central Texas, United States, and 13-year dripwater from Borneo, Malaysia) facilitates a tiered intermodel comparison approach. We used a hierarchy of PSMs of varying complexity to evaluate the fidelity of PSMs in capturing isotope hydrology. For Texas caves, which are located in subtropical to sub-arid regions, we show that the most simplified model (RM) can capture the mean values of cave dripwater $\delta^{18}O$, but fails to simulate the amplitudes of dripwater $\delta^{18}O$ variability. Conversely, other IC models, PRYSM, SAS, and Karstolution, can simulate the variance of dripwater $\delta^{18}O$ and major excursions of $\delta^{18}O$ well, with RMSEs close to reported analytical (measurement) error (±0.3‰). The well-mixed mode of PRYSM is more suitable for diffuse-type drip sites, and the advection-dispersion mode is suitable for conduit-type drip sites. For the Borneo caves (representing a tropical, humid climate), the RM model simulates cave dripwater $\delta^{18}O$ with similar RMSE to those of IC models. This is likely due to the wet climate and short residence time of water in the vadoze zone. The short residence time in these caves limits the requirement for the model representation of complex karst processes, which "lowers the bar" for models to simulate dripwater $\delta^{18}O$ with accuracy.

We envision that these results will help guide model-user choices in selecting an appropriate speleothem model for a cave-related study. Firstly, if the residence time and mean climate of a given cave or set of caves are well-constrained via cave monitoring, that information can be used to guide the selection of an appropriate PSM. If cave dripwater $\delta^{18}O$ responds to precipitation $\delta^{18}O$ quickly (i.e., short residence time <6 months) and the cave is located in a wet, tropical climate, the RM model is a defensible choice for simulating dripwater $\delta^{18}O$. By contrast, caves with long residence times (>6 months) likely require intermediate speleothem PSMs like PRYSM to simulate speleothem $\delta^{18}O$. PRYSM also only requires inputs of precipitation amount and precipitation $\delta^{18}O$, and contains fewer parameters to tune compared with SAS and Karstolution. More complex models like SAS (with a carbonate fractionation model like ISOLUTION) and Karstolution can most accurately simulate speleothem $\delta^{18}O$ (with RMSEs close to

analytical errors) but require tuning large sets of parameters. Secondly, selecting a PSM depends on the user's scientific application and question. Investigations of highly-constrained cave sites with long-term cave monitoring data may uniquely benefit from the use of complex models such as SAS and Karstolution, especially in water-scarce regions where high-level constraints on local hydrology are sorely needed. In addition, to thoroughly understand cave/karst processes in a particular cave, Karstolution is useful due to the greater number of physical processes simulated. However, for applications simulating global pseudo-speleothem $\delta^{18}O$ using climate model simulations as inputs, PRYSM is recommended given its relative ease of tuning and few parameters; despite its simplicity, PRYSM simulates the necessary physical processes in karst systems yielding realistic simulations of dripwater $\delta^{18}O$. Finally, for the simulation of global pseudo-speleothem $\delta^{18}O$, we note that PRYSM is not the only option. Global karst hydrology models like VarKarst-R can also simulate large-scale karstic groundwater recharge and incorporate karst processes.

This paper delineates a framework for the broader paleoclimate data-model comparison community to identify and distinguish between the various PSMs that have recently been published. Given the recent advancements of global datasets of paleoclimate records (Emile-Geay et al., 2017; Atsawawaranunt et al., 2018; Konecky et al., 2020), isotope-enabled climate models (Schmidt et al., 2005; Risi et al., 2012; Dee et al., 2015b; Yoshimura, 2015; Nusbaumer et al., 2017; Brady et al., 2019; Stevenson et al., 2019), and paleoclimate reanalysis products employing novel data assimilation techniques (Hakim et al., 2016; Steiger et al., 2018; Tardif et al., 2019), the necessity of suitable PSMs bridging climate variables and paleoclimate proxies is ever-growing. We envision broader use of PSMs in paleoclimate data-model comparison and cutting-edge applications in paleoclimate data assimilation (Comboul et al., 2015; Dee et al., 2016; Steiger et al., 2017), expanding the retrieval of climate signals from both paleoclimate proxies and model simulations in a common language.

Author statement

Jun Hu: Investigation, Methodology, Formal analysis, Writing – Original draft preparation. **Sylvia G. Dee:** Conceptualization, Software, Supervision, Writing – Reviewing and Editing. **Corinne I. Wong:** Conceptualization, Investigation, Writing – Original draft preparation. **Ciaran J. Harman:** Software, Writing – Reviewing and Editing. **Jay L. Banner:** Supervision, Writing – Reviewing and Editing. **Kendra E. Bunnell:** Investigation.

Declaration of competing interest

The authors declare that they have no known competing financial interests or personal relationships that could have appeared to influence the work reported in this paper.

Acknowledgements

The authors acknowledge postdoctoral funding from the Department of Earth, Environmental, and Planetary Sciences at Rice University. Research conducted at The University of Texas at Austin was facilitated by many students in the Banner research group and supported through the PaleoTexas project of the Planet Texas 2050 initiative and the F. M. Bullard Professorship. The authors especially thank the members of the Past Global Changes PAGES-DAPS (Data Assimilation and Proxy System Modeling) working group for initiating helpful conversations and spurring working groups on PSM inter-model comparisons and applications during a workshop held in May 2019. We thank Michael Evans in particular for suggesting the importance of evaluating a hierarchy of models of varying complexity.

Appendix A. Supplementary data

Supplementary data to this article can be found online at https://doi.org/10.1016/j.quascirev.2021.106799.

References

Atsawawaranunt, K., Comas-Bru, L., Amirnezhad Mozhdehi, S., Deininger, M., Harrison, S.P., Baker, A., Boyd, M., Kaushal, N., Ahmad, S.M., Brahim, Y.A., Arienzo, M., Bajo, P., Braun, K., Burstyn, Y., Chawchai, S., Duan, W., Hatvani, I.G., Hu, J., Kern, Z., Labuhn, I., Lachniet, M., Lechleitner, F.A., Lorrey, A., Pérez-Mejías, C., Pickering, R., Scroxton, N., SISAL Working Group Members, 2018. The SISAL database: a global resource to document oxygen and carbon isotope records from speleothems. Earth Syst. Sci. Data 10 (3), 1687–1713. https://doi.org/10.5194/essd-10-1687-2018.

Baker, A., Bradley, C., 2010. Modern stalagmite $\delta^{18}O$: instrumental calibration and forward modelling. Global Planet. Change 71 (3–4), 201–206.

Baker, A., Bradley, C., Phipps, S.J., 2013. Hydrological modeling of stalagmite $\delta^{18}O$ response to glacial-interglacial transitions. Geophys. Res. Lett. 40 (12), 3207–3212.

Baker, A., Hartmann, A., Duan, W., Hankin, S., Comas-Bru, L., Cuthbert, M.O., Treble, P.C., Banner, J., Genty, D., Baldini, L.M., Bartolomé, M., Moreno, A., Pérez-Mejías, C., Werner, M., 2019. Global analysis reveals climatic controls on the oxygen isotope composition of cave drip water. Nat. Commun. 10 (1), 1–7.

Bar-Matthews, M., Ayalon, A., Kaufman, A., Wasserburg, G.J., 1999. The Eastern Mediterranean paleoclimate as a reflection of regional events: soreq cave, Israel. Earth Planet Sci. Lett. 166 (1–2), 85–95.

Brady, E., Stevenson, S., Bailey, D., Liu, Z., Noone, D., Nusbaumer, J., Otto-Bliesner, B.L., Tabor, C., Tomas, R., Wong, T., Zhang, J., Zhu, J., 2019. The connected isotopic water cycle in the Community Earth System Model version 1. J. Adv. Model. Earth Syst. 11, 2547–2566. https://doi.org/10.1029/2019MS001663.

Bunnell, K.E., 2019. The Response of Central Texas Cave Drip Sites to Extreme Events: Implications for Paleoclimatology. Master's thesis. the University of Texas at Austin, Austin, United States. https://doi.org/10.26153/tsw/2799.

Carolin, S.A., Cobb, K.M., Adkins, J.F., Clark, B., Conroy, J.L., Lejau, S., Malang, J., Tuen, A.A., 2013. Varied response of western Pacific hydrology to climate forcings over the last glacial period. Science 340 (6140), 1564–1566. https://doi.org/10.1126/science.1233797.

Carolin, S.A., Cobb, K.M., Lynch-Stieglitz, J., Moerman, J.W., Partin, J.W., Lejau, S., Malang, J., Clark, B., Tuen, A.A., Adkins, J.F., 2016. Northern Borneo stalagmite records reveal West Pacific hydroclimate across MIS 5 and 6. Earth Planet Sci. Lett. 439, 182–193.

Cheng, H., Edwards, R.L., Broecker, W.S., Denton, G.H., Kong, X., Wang, Y., Zhang, R., Wang, X., 2009. Ice age terminations. Science 326 (5950), 248–252. https://doi.org/10.1126/science.1177840.

Cheng, H., Edwards, R.L., Shen, C.-C., Polyak, V.J., Asmerom, Y., Woodhead, J., Hellstrom, J., Wang, Y., Kong, X., Spötl, C., Wang, X., Alexander, E.C., 2013. Improvements in ^{230}Th dating, ^{230}Th and 234 U half-life values, and U–Th isotopic measurements by multi-collector inductively coupled plasma mass spectrometry. Earth Planet Sci. Lett. 371–372, 82–91. https://doi.org/10.1016/j.epsl.2013.04.006.

Cheng, H., Edwards, R.L., Sinha, A., Spötl, C., Yi, L., Chen, S., Kelly, M., Kathayat, G., Wang, X., Li, X., Kong, X., Wang, Y., Ning, Y., Zhang, H., 2016. The Asian monsoon over the past 640,000 years and ice age terminations. Nature 534 (7609), 640–646. https://doi.org/10.1038/nature18591.

Cheng, H., Sinha, A., Wang, X., Cruz, F.W., Edwards, R.L., 2012. The global paleomonsoon as seen through speleothem records from asia and the americas. Clim. Dynam. 39 (5), 1045–1062.

Comboul, M., Emile-Geay, J., Hakim, G.J., Evans, M.N., 2015. Paleoclimate sampling as a sensor placement problem. J. Clim. 28 (19), 7717–7740.

Cruz Jr., F.W., Karmann, I., Viana Jr., O., Burns, S.J., Ferrari, J.A., Vuille, M., Sial, A.N., Moreira, M.Z., 2005. Stable isotope study of cave percolation waters in subtropical Brazil: implications for paleoclimate inferences from speleothems. Chem. Geol. 220 (3–4), 245–262.

Dee, S., Emile-Geay, J., Evans, M.N., Allam, A., Steig, E.J., Thompson, D.M., 2015a. PRYSM: an open-source framework for PRoxY System Modeling, with applications to oxygen-isotope systems. J. Adv. Model. Earth Syst. 7 (3), 1220–1247. https://doi.org/10.1002/2015MS000447.

Dee, S., Noone, D., Buenning, N., Emile-Geay, J., Zhou, Y., 2015b. SPEEDY-IER: a fast atmospheric GCM with water isotope physics. J. Geophys. Res.: Atmosphere 120 (1), 73–91. https://doi.org/10.1002/2014JD022194.

Dee, S.G., Parsons, L.A., Loope, G.R., Overpeck, J.T., Ault, T.R., Emile-Geay, J., 2017. Improved spectral comparisons of paleoclimate models and observations via proxy system modeling: implications for multi-decadal variability. Earth Planet Sci. Lett. 476 (Suppl. C), 34–46. https://doi.org/10.1016/j.epsl.2017.07.036.

Dee, S.G., Steiger, N.J., Emile-Geay, J., Hakim, G.J., 2016. On the utility of proxy system models for estimating climate states over the Common Era. J. Adv. Model. Earth Syst. 8 (3), 1164–1179.

Deininger, M., Fohlmeister, J., Scholz, D., Mangini, A., 2012. Isotope disequilibrium effects: the influence of evaporation and ventilation effects on the carbon and oxygen isotope composition of speleothems – a model approach. Geochem. Cosmochim. Acta 96, 57–79.

Duan, W., Ruan, J., Luo, W., Li, T., Tian, L., Zeng, G., Zhang, D., Bai, Y., Li, J., Tao, T., Zhang, P., Baker, A., Tan, M., 2016. The transfer of seasonal isotopic variability between precipitation and drip water at eight caves in the monsoon regions of China. Geochem. Cosmochim. Acta 183, 250–266.

Ellis, S.A., Cobb, K.M., Moerman, J.W., Partin, J.W., Bennett, A.L., Malang, J., Gerstner, H., Tuen, A.A., 2020. Extended cave drip water time series captures the 2015–2016 El Niño in northern Borneo. Geophys. Res. Lett. 47, e2019GL086363 https://doi.org/10.1029/2019GL086363.

Emile-Geay, J., McKay, N.P., Kaufman, D.S., Von Gunten, L., Wang, J., Anchukaitis, K.J., others, 2017. A global multiproxy database for temperature reconstructions of the Common Era. Scientific Data 4, 170088.

Evans, M.N., Tolwinski-Ward, S.E., Thompson, D.M., Anchukaitis, K.J., 2013. Applications of proxy system modeling in high resolution paleoclimatology. Quat. Sci. Rev. 76, 16–28. https://doi.org/10.1016/j.quascirev.2013.05.024.

Feng, W., Casteel, R.C., Banner, J.L., Heinze-Fry, A., 2014. Oxygen isotope variations in rainfall, drip-water and speleothem calcite from a well-ventilated cave in Texas, USA: assessing a new speleothem temperature proxy. Geochem. Cosmochim. Acta 127, 233–250.

Gelaro, R., McCarty, W., Suárez, M., Todling, R., Molod, A., Takacs, L., Randles, C.A., Darmenov, A., Bosilovich, M.G., Reichle, R., Wargan, K., Coy, L., Cullather, R., Draper, C., Akella, S., Buchard, V., Conaty, A., da Silva, A.M., Gu, W., Kim, G., Koster, R., Lucchesi, R., Merkova, D., Nielsen, J.E., Partyka, G., Pawson, S., Putman, W., Rienecker, M., Schubert, S.D., Sienkiewicz, M., Zhao, B., 2017. The Modern-Era Retrospective Analysis for Research and Applications, Version 2 (MERRA-2). J. Clim. 30 (14), 5419–5454. https://doi.org/10.1175/JCLI-D-16-0758.1.

Gelhar, L.W., Wilson, J.L., 1974. Ground-water quality modeling. Groundwater 12 (6), 399–408.

Hakim, G.J., Emile-Geay, J., Steig, E.J., Noone, D., Anderson, D.M., Tardif, R., Steiger, N., Perkins, W.A., 2016. The last millennium climate reanalysis project: framework and first results. J. Geophys. Res.: Atmosphere 121, 6745–6764. https://doi.org/10.1002/2016JD024751.

Harman, C.J., 2015. Time-variable transit time distributions and transport: theory and application to storage-dependent transport of chloride in a watershed. Water Resour. Res. 51 (1), 1–30.

Hartmann, A., Goldscheider, N., Wagener, T., Lange, J., Weiler, M., 2014. Karst water resources in a changing world: review of hydrological modeling approaches. Rev. Geophys. 52 (3), 218–242.

Hartmann, A., Gleeson, T., Rosolem, R., Pianosi, F., Wada, Y., Wagener, T., 2015. A large-scale simulation model to assess karstic groundwater recharge over Europe and the Mediterranean. Geosci. Model Dev. (GMD) 8, 1729–1746. https://doi.org/10.5194/gmd-8-1729-2015.

Hulewicz, M., 2015. Physical and Geochemical Response in Cave Drip Waters to Recent Drought, Central Texas, USA: Implications for Drought Reconstruction Using Speleothems. Master's thesis. the University of Texas at Austin, Austin, United States.

James, E.W., Banner, J.L., Hardt, B., 2015. A global model for cave ventilation and seasonal bias in speleothem paleoclimate records. G-cubed 16, 1044–1051. https://doi.org/10.1002/2014GC005658.

Kirchner, J.W., Feng, X., Neal, C., 2001. Catchment-scale advection and dispersion as a mechanism for fractal scaling in stream tracer concentrations. J. Hydrol. 254 (1), 82–101.

Konecky, B.L., McKay, N.P., Churakova (Sidorova), O.V., Comas-Bru, L., Dassié, E.P., DeLong, K.L., von Gunten, L., 2020. The Iso2k Database: a global compilation of paleo-$\delta^{18}O$ and $\delta^{2}H$ records to aid understanding of Common Era climate. Earth Syst. Sci. Data Discuss. 2020, 1–49. https://doi.org/10.5194/essd-2020-5.

Koster, R.D., Suarez, M.J., Ducharne, A., Stieglitz, M., Kumar, P., 2000. A catchment-based approach to modeling land surface processes in a general circulation model: 1. Model structure. J. Geophys. Res. 105, 24809–24822. https://doi.org/10.1029/2000JD900327.

Lambert, W.J., Aharon, P., 2011. Controls on dissolved inorganic carbon and $\delta^{13}C$ in cave waters from DeSoto Caverns: implications for speleothem $\delta^{13}C$ assessments. Geochem. Cosmochim. Acta 75 (3), 753–768.

Mazzilli, N., Guinot, V., Jourde, H., Lecoq, N., Labat, D., Arfib, B., Baudement, C., Danquigny, C., Dal Soglio, L., Bertin, D., 2019. KasrtMod: a modelling platform for rainfall-discharge analysis and modelling dedicated to karst systems. Environ. Model. Software 122, 103927. https://doi.org/10.1016/j.envsoft.2017.03.015.

McDermott, F., 2004. Palaeo-climate reconstruction from stable isotope variations in speleothems: a review. Quat. Sci. Rev. 23 (7–8), 901–918. https://doi.org/10.1016/j.quascirev.2003.06.021.

McGuire, K.J., McDonnell, J.J., 2006. A review and evaluation of catchment transit time modeling. J. Hydrol. 330 (3–4), 543–563. https://doi.org/10.1016/j.jhydrol.2006.04.020.

Menne, M.J., Durre, I., Vose, R.S., Gleason, B.E., Houston, T.G., 2012. An overview of the global historical Climatology network-daily database. J. Atmos. Ocean. Technol. 29, 897–910. https://doi.org/10.1175/JTECH-D-11-00103.1.

Moerman, J.W., Cobb, K.M., Partin, J.W., Meckler, A.N., Carolin, S.A., Adkins, J.F., Lejau, S., Malang, J., Clark, B., Tuen, A.A., 2014. Transformation of ENSO-related rainwater to dripwater $\delta^{18}O$ variability by vadose water mixing. Geophys. Res. Lett. 41 (22), 7907–7915. https://doi.org/10.1002/2014GL061696.

Nusbaumer, J., Wong, T.E., Bardeen, C., Noone, D., 2017. Evaluating hydrological processes in the Community Atmosphere Model Version 5 (CAM5) using stable isotope ratios of water. J. Adv. Model. Earth Syst. 9 (2), 949–977. https://doi.org/10.1002/2016MS000839.

Oster, J.L., Montañez, I.P., Kelley, N.P., 2012. Response of a modern cave system to large seasonal precipitation variability. Geochem. Cosmochim. Acta 91, 92–108.

Pape, J.R., Banner, J.L., Mack, L.E., Musgrove, M., Guilfoyle, A., 2010. Controls on oxygen isotope variability in precipitation and cave drip waters, central Texas, USA. J. Hydrol. 385 (1–4), 203–215.

Partin, J., Quinn, T., Shen, C., Emile-Geay, J., Taylor, F., Maupin, C., Lin, K., Jackson, C.S., Banner, J.L., Sinclair, D.J., Huh, C.A., 2013. Multidecadal rainfall variability in South Pacific Convergence Zone as revealed by stalagmite geochemistry. Geology 41 (11), 1143–1146.

Partin, J.W., Jenson, J.W., Banner, J.L., Quinn, T.M., Taylor, F.W., Sinclair, D., Hardt, B., Lander, M.A., Bell, T., Miklavič, B., Jocson, J.M.U., Taboroši, D., 2012. Relationship between modern rainfall variability, cave dripwater, and stalagmite geochemistry in Guam, USA. G-cubed 13, Q03013. https://doi.org/10.1029/2011GC003930.

Reichle, R.H., Draper, C.S., Liu, Q., Girotto, M., Mahanama, S.P.P., Koster, R.D., De Lannoy, G.J.M., 2017. Assessment of MERRA-2 land surface hydrology estimates. J. Clim. 30, 2937–2960. https://doi.org/10.1175/JCLI-D-16-0720.1.

Risi, C., Noone, D., Worden, J., Frankenberg, C., Stiller, G., Kiefer, M., Funke, B., Walker, K., Bernath, P., Schneider, M., Wunch, D., Sherlock, V., Deutscher, N., Griffith, D., Wennberg, P.O., Strong, K., Smale, D., Mahieu, E., Barthlott, S., Hase, F., García, O., Notholt, J., Warneke, T., Toon, G., Sayres, D., Bony, S., Lee, J., Brown, D., Uemura, R., Strum, C., 2012. Process-evaluation of tropospheric humidity simulated by general circulation models using water vapor isotopologues: 1. Comparison between models and observations. J. Geophys. Res.: Atmosphere 117, D05303. https://doi.org/10.1029/2011JD016621.

Schmidt, G.A., Hoffmann, G., Shindell, D.T., Hu, Y., 2005. Modeling atmospheric stable water isotopes and the potential for constraining cloud processes and stratosphere-troposphere water exchange. J. Geophys. Res.: Atmosphere 110 (D21).

Smart, P.L., Friederich, H., 1986. Water movement and storage in the unsaturated zone of a maturely karstified aquifer, Mendip Hills, England. In: Paper Presented at the Conference on Environmental Problems in Karst Terrains and Their Solutions. Natl. Water Wells Assoc., Bowling Green, Ky.

Steiger, N.J., Smerdon, J.E., Cook, E.R., Cook, B.I., 2018. A reconstruction of global hydroclimate and dynamical variables over the Common Era. Scientific Data 5, 180086. https://doi.org/10.1038/sdata.2018.86.

Steiger, N.J., Steig, E.J., Dee, S.G., Roe, G.H., Hakim, G.J., 2017. Climate reconstruction using data assimilation of water isotope ratios from ice cores. J. Geophys. Res.: Atmosphere 122 (3), 1545–1568.

Stevenson, S., Otto-Bliesner, B., Brady, E., Nusbaumer, J., Tabor, C., Tomas, R., Noone, D.C., Liu, Z., 2019. Volcanic eruption signatures in the isotope-enabled last millennium ensemble. Paleoceanography and Paleoclimatology 34, 1534–1552. https://doi.org/10.1029/2019PA003625.

Tardif, R., Hakim, G.J., Perkins, W.A., Horlick, K.A., Erb, M.P., Emile-Geay, J., Anderson, D.M., Steig, E.J., Noone, D., 2019. Last Millennium Reanalysis with an expanded proxy database and seasonal proxy modeling. Clim. Past 15, 1251–1273. https://doi.org/10.5194/cp-15-1251-2019.

Treble, P.C., Bradley, C., Wood, A., Baker, A., Jex, C.N., Fairchild, I.J., Gagan, M.K., Cowley, J., Azcurra, C., 2013. An isotopic and modelling study of flow paths and storage in Quaternary calcarenite, SW Australia: implications for speleothem paleoclimate records. Quat. Sci. Rev. 64, 90–103.

Treble, P., Mah, M., Griffiths, A., Baker, A., Deininger, M., Kelly, B., Scholz, D., Hankin, S., 2019. Separating isotopic impacts of karst and in-cave processes from climate variability using an integrated speleothem isotope-enabled forward model. EarthArXiv. https://doi.org/10.31223/osf.io/j4kn6.

Vrugt, J.A., 2016. Markov chain Monte Carlo simulation using the DREAM software package: theory, concepts, and MATLAB implementation. Environ. Model. Software 75, 273–316. https://doi.org/10.1016/j.envsoft.2015.08.013.

Wackerbarth, A., Scholz, D., Fohlmeister, J., Mangini, A., 2010. Modelling the $\delta^{18}O$ value of cave drip water and speleothem calcite. Earth Planet Sci. Lett. 299 (3–4), 387–397.

Wang, Y., Cheng, H., Edwards, R.L., Kong, X., Shao, X., Chen, S., Wu, J., Jiang, X., Wang, X., An, Z., 2008. Millennial-and orbital-scale changes in the East Asian monsoon over the past 224,000 years. Nature 451 (7182), 1090–1093. https://doi.org/10.1038/nature06692.

Wang, Y.-J., Cheng, H., Edwards, R.L., An, Z., Wu, J., Shen, C.-C., Dorale, J.A., 2001. A high-resolution absolute-dated late Pleistocene monsoon record from Hulu Cave, China. Science 294 (5550), 2345–2348. https://doi.org/10.1126/science.1064618.

Wilusz, D.C., Harman, C.J., Ball, W.P., 2017. Sensitivity of catchment transit times to rainfall variability under present and future climates. Water Resour. Res. 53 (12), 10231–10256. https://doi.org/10.1002/2017WR020894.

Wong, C.I., Banner, J.L., Musgrove, M., 2011. Seasonal dripwater Mg/Ca and Sr/Ca variations driven by cave ventilation: implications for and modeling of speleothem paleoclimate records. Geochem. Cosmochim. Acta 75, 3514–3529. https://doi.org/10.1016/j.gca.2011.03.025.

Wong, C.I., Breecker, D.O., 2015. Advancements in the use of speleothems as climate archives. Quat. Sci. Rev. 127, 1–18.

Yoshimura, K., 2015. Stable water isotopes in Climatology, meteorology, and hydrology: a review. J. Meteorol. Soc. Jpn. 93 (5), 513–533.